International Journal of Applied Mathematics in Control Engineering 4 (2021) 127-134

Contents lists available at YXpublications

International Journal of Applied Mathematics in Control Engineering

Journal homepage: http://www.ijamce.com

Research on Pulsation Suppression of New High-Speed Two-Phase Switched Reluctance Motor

Linhou Yu*, Haonan Li

College of Information Science and Engineering, Hebei University of Science and Technology, Shijiazhuang, 050018, china

ARTICLE INFO

Article history:
Received 5 July 2021
Accepted 10 October 2021
Available online 15 October 2021

Keywords:
High-speed operation
Two-phase switched reluctance motor
Finite element analysis
Air gap
Torque ripple suppression

ABSTRACT

Aiming at the matters of high-speed two-phase switched reluctance motor (SRM) lacking self-starting ability and large torque ripple, a study on the optimization of the body structure of 8/4-pole switched reluctance motor is proposed. The mathematical model is used to analyze the structure of the motor. ANSOFT is used to fit the curve between the number of turns and the air gap, and the optimal solution is obtained under different number of turns and the size of air gap. The results from two dimensional finite element static simulation show that the parameter optimization improves the self-starting ability of the motor and significantly reduces the torque ripple.

1. Introduction

In the 1960s, with the birth of high-power thyristor, the research process of switched reluctance motor was greatly promoted. In just a few decades, switched reluctance motor (SRM) quickly occupied an important position in the field of motor because of its low cost, simple structure and high stability. The specific advantages are as follows.

(1) The structure of SR motor is simpler than that of squirrel cage asynchronous motor [1]. In literature [1], it is said that the biggest advantage of switched reluctance motor is that there is no winding on the rotor, so it will not produce problems such as unqualified quality when manufacturing squirrel cage asynchronous motor and easy bar breaking when starting and stopping frequently.

(2) Each phase works independently and the system has high stability. Document [2-3] describes the electromagnetic structure of the motor. Each phase winding and magnetic circuit are independent of each other and produce electromagnetic torque within a certain shaft angle range. Unlike in general motors, circular rotating magnetic field must be generated under the joint action of each winding and magnetic circuit before the motor can operate normally. From the controller structure, each phase winding is powered by an independent circuit, so it also works independently of each other.

(3) The power circuit is simple and reliable. The torque direction of switched reluctance motor is only related to the energization sequence, but independent of the direction of winding current, that is, only one direction of winding current is required, so the power circuit can achieve one power switch for each phase. Compared with the bidirectional current continuously flowing through the winding of induction motor, the power supply circuit of PWM inverter requires two power elements per phase. Therefore, the switched reluctance motor speed regulation system requires fewer power components than the PWM frequency converter power circuit, and the circuit structure is simple [4-5].

The structure of switched reluctance motor determines its optimization method. Its unique double salient structure and switching power supply lead to some disadvantages: on the one hand, the edge magnetic flux generated before the overlapping of stator teeth and rotor teeth causes the nonlinear change of current; On the other hand, the torque on SRM rotor is superimposed by pulse torque, and the synthetic torque is not a constant value. These two points lead to the inherent torque ripple of switched reluctance motor, especially at low speed. Therefore, minimizing torque ripple has become one of the important contents of SR motor optimization design.

From the perspective of common control strategies, torque distribution control can avoid large peak current, but it needs to control the two phases in the commutation area at the same time, occupying more control interface resources and high cost [5]. Fuzzy control and neural network are difficult to measure real-time dynamic torque, and sensors are expensive [6-7]. In reference [8],

* Corresponding author.
E-mail addresses: 526055394@qq.com (L. Yu)

iterative learning control has low requirements for motor magnetic characteristics, accuracy and controller, but it has high requirements for motor operating conditions, which is not conducive to maintaining the advantages of economy and high reliability of two-phase SR motor. The research on the motor body can avoid the disadvantages of high cost and poor practicability of the control strategy. Based on the improvement of T-shaped rotor teeth, document [9] reduces the torque ripple by reducing the radial force wave integral area. In reference [10], wide rotor stepping and adding permanent magnet are adopted for 4 / 2-pole and 4 / 4-pole SRM respectively, so that the motor has uneven air gap, changes its inductance curve and improves torque performance. Literature [11] adopts a new short flux path, which greatly reduces the loss of copper wire and iron core, and significantly improves the torque and efficiency of motor. At present, ontology research is mostly based on three-phase and above motors. Therefore, systematic optimization from the ontology level of two-phase motors is of great research significance to maintain the inherent advantages of two-phase motors.

Starting with the motor body, this paper designs the motor structure, winding turns, step air gap size, air gap angle and other parameters for comprehensive optimization and improvement, so as to suppress the motor torque ripple and improve its self-starting ability. According to the optimized motor parameters and step air gap, an external circuit based on angle position control is built for two-dimensional field circuit coupling simulation. The effectiveness of this method is proved by controlling the breaking frequency of electronic components in the external circuit and simulating the motor operation after parameter optimization.

2. SRM working principle and mathematical model

2.1 Basic principles of switched reluctance motors

The working principle of switched reluctance motor follows the principle of minimum reluctance, that is, the magnetic flux always closes along the path of minimum reluctance. Therefore, its structural principle is that the magnetic resistance of the magnetic circuit should change as much as possible when the rotor rotates. Therefore, switched reluctance motor adopts double salient pole structure of salient pole stator and salient pole rotor, and the number of poles of stator and rotor is different. The stator and rotor of switched reluctance motor are salient pole cogging structure. The stator and rotor cores are punched into slots of a certain shape by silicon steel sheets, and then laminated. The structure of stator and rotor punching sheets is shown in Figure 1.

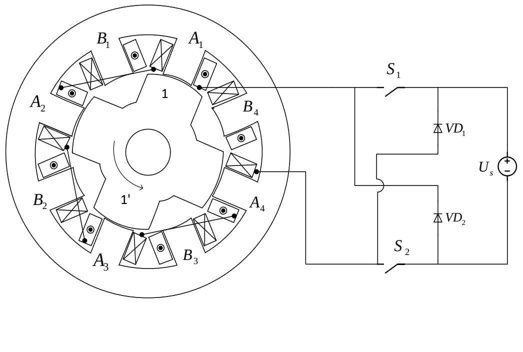

Fig. 1. Structural schematic diagram of two-phase switched reluctance motor

The above figure shows the 8/4-pole two-phase switched reluctance motor system specially designed for the rotor, including the motor body and drive control part. The 8 coils of the 8 salient poles of the stator are connected at intervals to form two-phase windings a and B. the connection mode of the 4 coils of each phase is mainly nsns. This connection mode has a short magnetic circuit, which is beneficial to reducing iron consumption. The rotor is of 4 salient pole iron core structure.

The main circuit of two-phase switched reluctance motor adopts asymmetric bridge circuit. Only the main circuit of phase A is shown in Figure 1. It can be seen that because it is a two-phase motor, there are only four power tubes, which is conducive to reducing the cost of motor drive system.

The figure above shows a pair of magnetic poles of stator phase a winding and its external circuit. When the phase a winding is energized, the stator magnetic field is generated. At this time, the air gap magnetoresistance of the closed circuit through which the main magnetic flux passes is large, and the tangential magnetic pull generated by the principle of minimum magnetoresistance makes the rotor rotate to the position where axis 11 'coincides with A_1A_3. The existence of the stepped air gap structure changes the generated inductance, so as to change the magnetoresistance accordingly. At the position shown in the figure, energize A → B → A in turn and rotate counterclockwise against the excitation sequence.

2.2 Mathematical model of switched reluctance motor

The operation theory of switched reluctance motor is essentially the same as that of other electromagnetic motor devices. It is the electromechanical conversion of electrical energy and mechanical energy. It can be regarded as a two port device with a pair of electrical ports and a pair of mechanical ports. Taking two-phase switched reluctance motor as an example, if some factors affecting loss and winding mutual inductance are not considered, the schematic diagram of SR motor drive system can be shown in Figure 2.

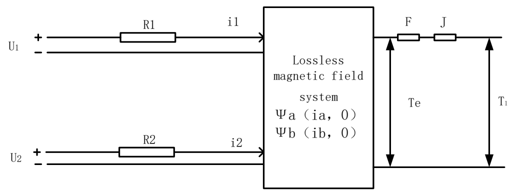

Fig. 2. Schematic diagram of two-phase SRM drive system

In Figure 2, j is the moment of inertia of SR motor rotor and load, $kg \cdot m^2$; B is viscous friction coefficient; Is the load torque, $N \cdot m$. From the perspective of mechanical electrical analysis, the differential equation describing the dynamic process of the electromechanical system shown in Fig. 2 can be composed of voltage equation, flux equation, mechanical motion equation and torque equation.

Figure 2 shows the moment of inertia of switched reluctance motor rotor and load, U_k is the stator phase winding voltage, where k = 1, 2;R_k is the resistance of stator phase winding, where k = 1, 2;i_k is the current of stator phase winding, where k = 1, 2;ψ_k is the stator phase winding voltage, where k = 1, 2; J is the moment of inertia, T_e is the load torque, K_ω is the viscous friction coefficient, T_l is the load torque, The differential equation describing the dynamic process of the electromechanical system shown in Fig. 2 can be composed of voltage equation, flux equation, mechanical motion equation and torque equation.

Voltage equation: according to the basic law of the circuit, the voltage applied to both ends of the windings of each phase of the stator is equal to the sum of the voltage drop of each phase of the stator and the induced electromotive force caused by the change of flux linkage. Therefore, the voltage balance equation of phase K of SRM can be written:

$$U_k = R_k i_k + \frac{d\Psi_k(\theta_k, i_k)}{dt} \quad (1)$$

In formula (1), U_k, i_k, R_k is the terminal voltage, current and resistance of the k-phase winding of the motor, θ_k is the rotor position angle of the k-phase of the motor, and $\psi_k(\theta_k, i_k)$ is the flux linkage of the k-phase winding of the motor.

Flux linkage equation: the flux linkage of each phase winding of SRM is a function of phase current and self inductance, other phase current and mutual inductance, and rotor position angle. Compared with self inductance, the mutual inductance between SRM phases is small. In order to facilitate analysis, the phase to phase inductance can be ignored in the calculation of motor. Therefore, the flux linkage equation can be written as

$$\Psi_k = L_k(\theta_k, i_k) i_k \quad (2)$$

In formula (2), $L_k(\theta_k, i_k)$ is the inductance of each phase, which is a function of phase current i_k and rotor position angle θ_k.

The following is the process of transforming formula (2) and deriving the partial differential of Ψ_k:

$$U_k = R_k i_k + \frac{\partial \Psi_k}{\partial i_k}\frac{di_k}{dt} + \frac{\partial \Psi_k}{\partial \theta}\frac{d\theta}{dt} \quad (3)$$

$$U_k = R_k i_k + \left(L_k + i_k \frac{\partial L_k}{\partial i_k}\right)\frac{di_k}{dt} + i_k \frac{\partial L_k}{\partial \theta}\omega \quad (4)$$

$$U_k = R_k i_k + e_t + e_m \quad (5)$$

In formula (5), $e_t$is the electromotive force induced by the change of flux linkage caused by current conversion, which is called transformer electromotive force. e_m is the electromotive force induced by the change of flux linkage in the winding caused by the change of rotor position, which is called moving electromotive force or motor electromotive force. e_m is directly related to the electromechanical energy conversion of SRM.

Mechanical motion equation: according to the mechanical principle, the mechanical motion equation of the rotor of SRM under electromagnetic torque T_e and load torque T_l can be written.

$$T_e = J\frac{d^2\theta}{dt^2} + K_\omega \frac{d\theta}{dt} + T_l \quad (6)$$

In formula (6), J is the moment of inertia of the system and K_ω is the friction coefficient. When the electromagnetic torque of the motor is inconsistent with the load torque acting on the motor shaft, the speed will change and produce angular acceleration.

It is expressed by $\frac{d\omega}{dt}$. Then$\omega = \frac{d\theta}{dt}$, the mechanical motion

equation can be transformed into the following formula.

$$T_e = J\frac{d\omega}{dt} + K_\omega \omega + T_l \quad (7)$$

When the SRM operates stably, $\frac{d\omega}{dt} = 0$, then

$$T_e = K_\omega \omega + T_l = K_\omega \frac{d\theta}{dt} + T_l \quad (8)$$

According to the law of energy conservation, electromagnetic torque can be expressed as a function of magnetic common energy (output mechanical energy). Without considering the resistance loss, core loss and mechanical loss caused by rotor rotation, the electrical energy W_e input to the winding shall be equal to the sum of magnetic field energy storage W_m and magnetic common energy W_f.

The correlation equation of SRM describes the relationship between electromechanical energy conversion process and electromagnetic torque. The energy conversion of SRM meets the law of energy conservation. Take the current flux change curve of one phase of SRM winding to describe the energy conversion process, as shown in Figure 3.

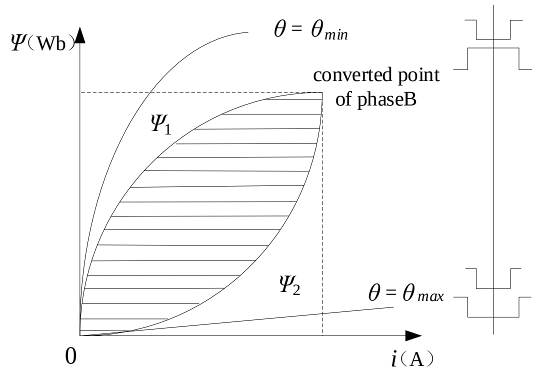

Fig. 3 curve of switched reluctance motor $\Psi - i$

The magnetization curves of the minimum and maximum reluctance positions correspond to $\theta = \theta_{min}$ and $\theta = \theta_{max}$ curves respectively. When the phase is on, the corresponding flux change curve is $\Psi_1 = \Psi_1(\theta, i)$. The current freewheeling in the relevant broken winding corresponds to $\Psi_2 = \Psi_2(\theta, i)$. In the process of motor rotation, the magnetic common energy W_f and magnetic energy storage W_m change nonlinearly. When one phase is on, it begins to rise along Ψ_1. When it reaches commutation point B, the winding flux reaches the maximum value. When the correlation is broken, the flux begins to fall along Ψ_2 and finally falls to zero.

Variation of magnetic common energy in the whole process:

$$\Delta W_f = \oint_\Omega \Psi di = \int_0^{ic} \Psi_2 \, di - \int_0^{ic} \Psi_1 \, di = \int \Psi_2 - \Psi_1 \, di \quad (9)$$

Variation of magnetic energy storage:

$$\Delta W_m = \oint_\Omega i(\Psi, \theta) d\Psi = \int_0^{\Psi c} i_2 \, d\Psi - \int_0^{\Psi c} i_1 \, d\Psi = \int i_2 - i_1 \, d\Psi \quad (10)$$

In formula (10), Ω represents the closed curve in Fig. 2; i_1 represents the inverse function $i_1 = i_1(\Psi, \theta)$ of flux linkage Ψ_1; i_2 represents the inverse function $i_2 = i_2(\Psi, \theta)$ of flux linkage Ψ_2.

From formula (9) and formula (10), it can be obtained that W_f and W_m are equal in size and are the shaded area, so:

$$\Delta W_f = -W_m \quad (11)$$

Since the change of magnetic common energy is the same as that of magnetic storage energy, and the change of magnetic common energy is the same as that of mechanical energy ΔW_a, it can be deduced that:

$$\Delta W_f = -W_m = \Delta W_a \quad (12)$$

According to the electromechanical energy conversion principle $\Delta W_a = T_{avg}\Delta\theta$,$T_{avg}$ is the average torque within the rotor rotation angle of $\Delta\theta$, so:

$$T_{avg} = \frac{\Delta W_f}{\Delta\theta} = -\frac{W_m}{\Delta\theta} = \frac{\Delta W_a}{\Delta\theta} \quad (13)$$

According to the method of taking limit in mathematics, it is deduced that the instantaneous torque at any point α on the closed curve is:

$$T_\alpha = \left.\frac{\partial W'}{\partial \theta}\right|_{i=const} = -\left.\frac{\partial W_f}{\partial \theta}\right|_{\Psi=const} \quad (14)$$

For formula (14), the instantaneous torque integral is averaged in one cycle to obtain the average torque. When evaluating the torque performance, the calculation of the average torque is very meaningful. The average output torque considering the symmetry of the motor winding is:

$$T = \frac{mN_r}{2\pi}\int_0^{\frac{2\pi}{N_r}} T_\alpha(\theta, i(\theta))\,d\theta = \frac{mN_r}{2\pi}\int_0^{\frac{2\pi}{N_r}}\int_0^{i(\theta)} \frac{\partial W_m(\theta,\xi)}{\partial \theta}\xi d\xi d\theta \quad (15)$$

In formula (15), ξ is the intermediate variable of phase current, m is the number of phases of SRM, and N_r is the number of rotor teeth of SRM.

To sum up, the basic relations of switched reluctance motor are formula (5), formula (8) and formula (15). In theory, the established mathematical model of switched reluctance motor can accurately describe the electromechanical relationship of motor, but some variables are not easy to obtain, so there are different simplification methods in practical analysis.

3. Determination of the basic structure of the motor

3.1 Two-phase 8/4-pole switched reluctance motor

The traditional 4/2-pole two-phase switched reluctance motor has a small number of stator and rotor poles, resulting in uneven radial force distribution, and the inherent pulsation of the motor makes the vibration and noise problem more prominent. Increasing the number of stator and rotor poles can reduce torque ripple. Considering the difficulty and cost of motor processing, an 8/4-pole motor is selected. Figure 4 is a structural diagram of a two-phase 8/4-pole switched reluctance motor. The motor shown in the figure has 4 asymmetrical rotors, of which a pair of rotor pole arcs are wide, and 8 concentrated winding coils on the stator poles form two phases A and B. This structure allows the motor to have an uneven air gap to change the inductance distribution. Reduced torque ripple.

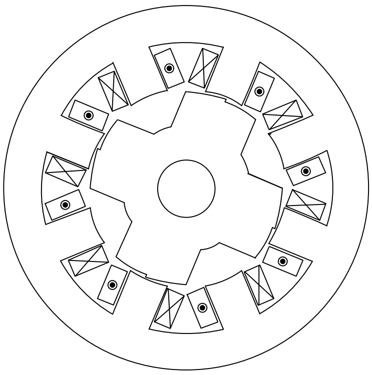

Fig. 4. Two-phase 8/4 pole switched reluctance motor structure diagram

3.2 Determination of motor performance requirements and size

The motor based on the application background of high-speed vacuum cleaners should meet the requirements of high enough speed, rated power and as small as possible. For this reason, a 1.5 KW, 220 V two-phase 8/4-pole motor is selected as a prototype. The basic dimensions of the motor are shown in Table 1. Show. The motor load torque is estimated to be 0.2 N · m when the motor is idling. At this time, the motor speed should be higher than 30000 r/min.

Tab. 1. Motor basic size

Motor parameters	Value
Rated power (kW)	1.5
Single-phase AC voltage (V)	220
Rotation speed at 0.2 load (r/min)	＞30 000
Stator outer diameter (mm)	102
Iron core length (mm)	≤50
Rotor inner diameter (mm)	24

The ratio of the core length to the stator outer diameter is usually defined as the slenderness ratio λ. According to the empirical value λ =0.5~3.0, D_s =102 mm is known, and L_{Fe} is finally determined to be 50 mm to ensure the capacity margin of the motor. The stator and rotor outer diameter ratio D_a/D_s of a switched reluctance motor is commonly designed with a ratio of 0.5 to 0.6. Because the motor has a high set speed and must maintain a certain mechanical strength, the rotor outer diameter is designed to be 55 mm. Considering the size of the magnetic density of the stator yoke and the influence of magnetic saturation on noise, the thickness of the stator yoke is selected as 10 mm. The motor design scheme is shown in Table 2.

Tab. 2. Motor design scheme

Motor parameters	Value
Thickness of stator yoke (mm)	10
Outer diameter of rotor (mm)	55
Stator pole arc θ_s (°)	22.5
Winding turns (turns)	38
Wire gauge	1×1.25
Rotor pole arc $\theta_{\delta_c}+\theta_{\delta}$ (°)	45

If only considering the structure and size of the two-phase switched reluctance motor, the performance of the motor cannot be effectively improved, and the number of winding turns and the air gap angle have a greater impact on the torque ripple of the motor, so these two parameters need to be further optimized.

4. Effect of structural parameters on torque ripple

4.1 determination of motor winding turns

The determination of the number of turns of the switched reluctance motor is affected by the phase current, and the form of the phase current is affected by the motor speed [12]. Set the current amplitude to I_m and the conduction width of each phase to θ_m, then:

$$T_e = \frac{1}{2}i^2\frac{\Delta L}{\Delta\theta} = \frac{1-k}{2}I_m^2\frac{L_{max}}{\theta_w} \quad (16)$$

In the formula, $\Delta L = L_{max} - L_{min} = L_{max}(1-k)$, K is the proportional coefficient, $\Delta\theta = \theta_w$

Because the two diametrically opposed windings are connected in series and the number of turns of each winding is N, the maximum inductance of the phase winding is:

$$L_{max} = 2N^2\lambda_{max} \quad (17)$$

In the formula, λ_{max} is the maximum permeance, when the motor structure is determined, λ_{max} is a fixed value. Simultaneous formulas (16) and (17) neglect other interference factors when running at low speed. The current is controlled by chopping and it is approximately a square wave, I_m is equal to the chopping limit, and the motor output torque is proportional to the square of the winding turns.

When the motor is running at high speed, the phase current is in the form of single pulse. When ω increases, $di/d\theta$ decreases. Therefore, once ω increases to a certain extent, and the maximum value of the phase current is less than the chopping limit I_m, the current of the motor works in the single pulse mode.

In the single pulse mode, assuming that ω is constant, the rise time T_1 of the phase current is a constant value. The maximum value of the phase current is:

$$I_{max} = \frac{U_S T_1}{K L_{max}} \tag{18}$$

From formulas (17) and (18), the maximum phase current is inversely proportional to the square of the winding turns. Therefore, a reasonable choice of winding turns can increase the maximum phase current, thereby increasing the motor output torque. The equation of motor winding turns is:

$$N = \frac{3.04 N_r U \theta_c}{n B_\delta D_a l_\delta} \tag{19}$$

In the formula, N_r is the number of rotors; θ_c is the conduction angle; B_δ is the preselected value of electromagnetic load; n is the speed; l_δ is the length of the winding wire.

Considering comprehensively, the design of the number of turns of the phase winding must take into account both current and speed. Taking into account the influence of the power, torque and size of the switched reluctance motor, the number of turns of the winding is initially calculated as 35 turns by formula (19).

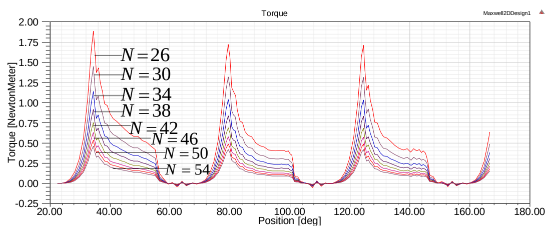

Fig. 5. Torque waveform at different turns

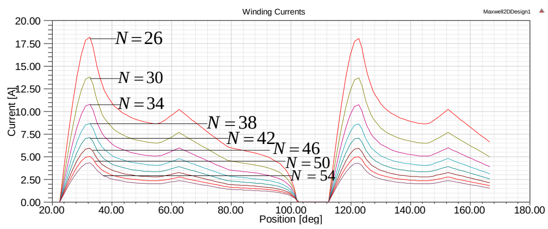

Fig. 6. Current waveforms at different turns

Figures 5 and 6 show the effects of different turns on torque and current. Taking into account the application of the motor and the appropriate slot full rate, the number of winding turns is 38.

4.2 design of stepped air gap structure

SRM produces reluctance electromagnetic torque due to the distortion of the magnetic field, which is not a constant torque [13]. Ignoring the coupling effect between phases, when the single-phase stator winding is turned on:

$$T_e = \frac{1}{2} k i^2 \frac{L_{max}}{\theta} \tag{20}$$

In the formula, $k = 1 - L_{min}/L_{max}$, usually $0.07 \ll L_{min}/L_{max} \ll 0.18$, θ is the rotor position angle, i is the phase current, L_{max} is the maximum inductance of the stator and rotor aligned positions, $L_{max} = N^2/R_g$, N is the number of winding turns.

The breath reluctance is $R_g = 2\delta/(D_s/2 \cdot L \cdot \theta \cdot \mu_0)$, D_s is the outer diameter of the stator, μ_0 is the air permeability, and δ is the first air gap. Substituting L_{max} and R_g into equation (20), we get:

$$T_e = \frac{\mu_0 k N^2 D_s L}{8\delta} i^2 \tag{21}$$

Suppose the air gap is a variable, and the torque is derived from the air gap:

$$\frac{dT_e}{d\delta} = -\frac{\mu_0 k N^2 D_s L i^2}{8} \frac{1}{\delta^2} \tag{22}$$

From formulas (21) and (22), it can be seen that there is an inverse proportional relationship between the first and second powers of the torque and the air gap. The change of the air gap can be changed by improving the stator and rotor tooth structure to obtain a structure that produces the smallest torque ripple. .

SRM torque pulsation is caused by the resonance of the phase current harmonic frequency and the stator natural frequency. Reducing the air gap can control the phase current waveform and weaken the harmonic component of the stator resonance. However, the reduction of the air gap is affected by machining and vibration and noise. Generally, the air gap of a small motor should be greater than 0.25 mm. Considering the stable operation and assembly of the motor, the air gap δ of the two-phase SR motor is set to 0.3 mm.

In the article, the rotor surface of the two-phase switched reluctance motor adopts an asymmetrical stepped air gap structure, which can eliminate the torque dead zone, reduce torque ripple, and improve the output efficiency of the motor. Figure 7 shows a two-phase 8/4-pole SRM air gap model, where δ_e is the stepped air gap, and θ_{δ_e} is the angle of the rotor pole arc corresponding to δ.

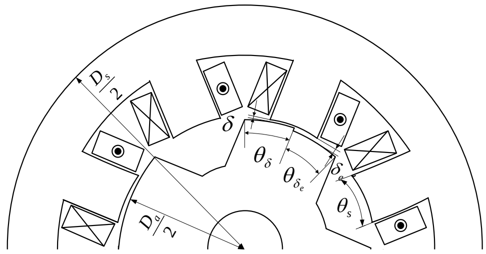

Fig. 7. Two-phase 8/4-pole SRM air gap model

On the basis of determining the main dimensions of the motor, finite element simulations are performed on different stepped air gaps δ_e and rotor pole arc angles θ_{δ_e}. As shown in the static torque curve in Figure 8, the intersection point of A and B is the minimum starting torque. The height of this point represents the strength of the self-starting ability. Therefore, analysis is made for factors such as the minimum starting torque and torque ripple. To determine the appropriate δ_e and θ_{δ_e}.

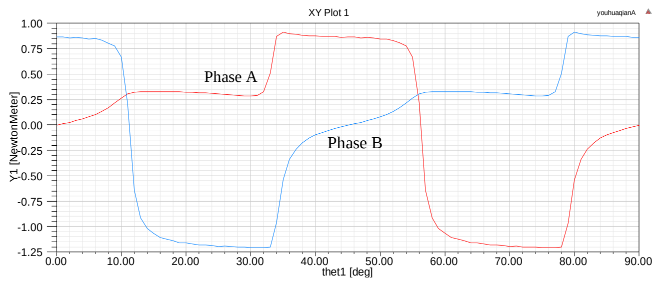

Fig. 8. Static torque curve

The design of SRM requires a higher starting torque and a smaller starting current, so a constant phase current of 5 A is passed in, and the simulation waveform of the static torque of the motor is obtained by changing θ_{δ_e} at different δ_e as shown in the curve in Fig. 9.

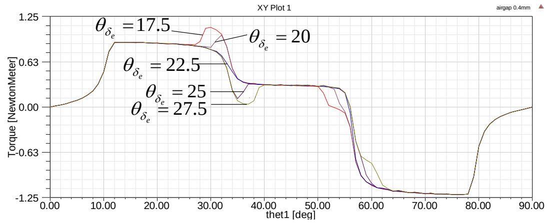

a) $\delta_e=0.4$

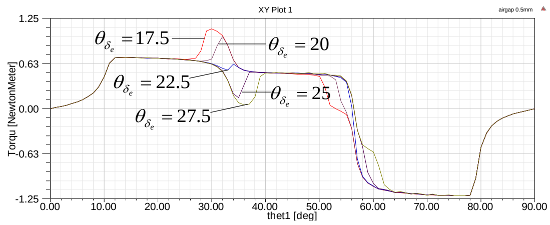

b) $\delta_e=0.5$

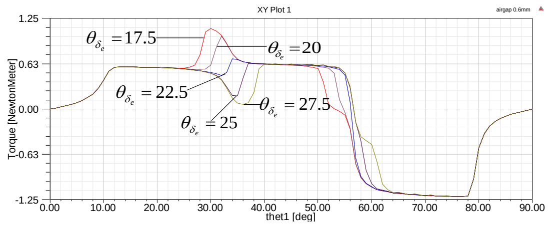

c) $\delta_e=0.6$

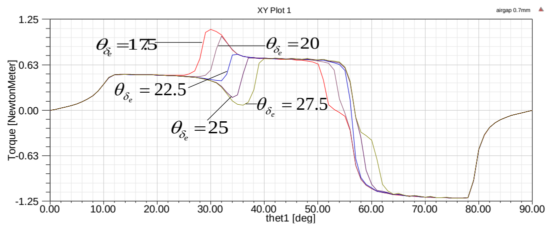

d) $\delta_e=0.7$

Fig. 9. Simulation waveform of motor static torque at different δ_e

As shown in Figure 9, with the increase of δ_e, the waveform of static torque gradually changes from high left to low right to low left and high right, and it is the smoothest when δ_e=0.6; the static torque difference between various angles gradually Becomes larger, and the fluctuation range is the smallest when θ_{δ_e}=22.5°.

Through analysis and further simulation verification, the stepped air gap of the motor is determined to be δ_e=0.55 and θ_{δ_e}=22.5°. Figure 10 shows the static torque waveform under this condition. In the figure, the motor has a minimum starting torque of about 0.35 N·m, which meets the motor's self-starting requirements and has good smoothness.

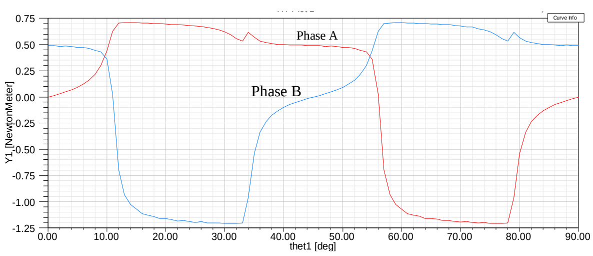

Fig. 10. A and B two-phase static torque simulation waveforms at δ_e=0.55, θ_{δ_e}=22.5°

5. Determination of the basic structure of the motor

Through the demonstration of the motor body scheme, Ansoft / Maxwell 2D is used for two-dimensional field circuit coupling simulation. The design speed of 30 000 r/min belongs to high speed, so the external circuit adopts angle control strategy. The external circuit is the synchronous joint simulation of the motor drive system with the finite element simulation by controlling the parameters such as diode breaking time and switching frequency. The driving circuit adopts asymmetric half bridge structure, and each phase winding adopts two switches for driving control.

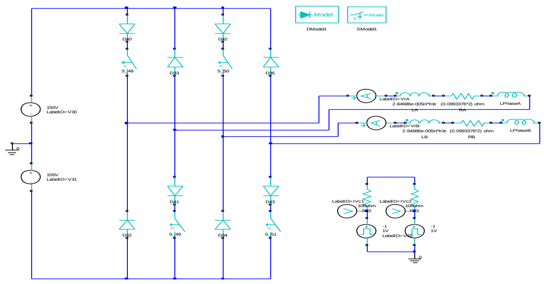

Fig. 11. Drive circuit

The intensity of the magnetic field can be judged by judging the magnetic flux density, and the magnetic lines of force when the stator and rotor poles are aligned and not aligned under the same current are collected. It is found that when the stator and rotor positions coincide, the magnetic field lines are the densest, and the stator and rotor are most likely to be saturated. Therefore, reducing the peak value at the aligned position is very helpful to improve the torque ripple of the motor. The stator and rotor magnetic field lines are distributed as shown in Figure 12.

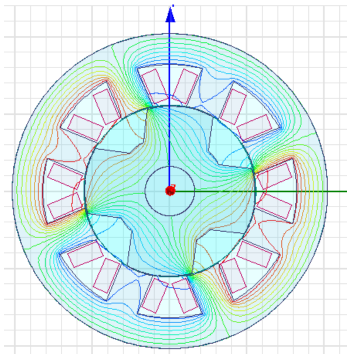

a) Not aligned

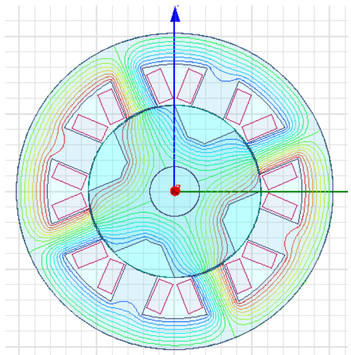

b) Align

Fig. 12. SRM magnetic field lines in different positions

The winding turns and air gap of the traditional two-phase switched reluctance motor have the greatest impact on the torque ripple. This compares the conventional vacuum cleaner motor with 35 turns and an air gap of 0.3 mm. From Fig. 13, it can be found that the speed difference between before and after the improvement of the motor is not large, but the fluctuation of the motor before and after the improvement is slightly larger at first than after the improvement, and then they all tend to be stable. The improved motor speed is slightly higher than before, which is more conducive to the application of ultra-high-speed occasions.

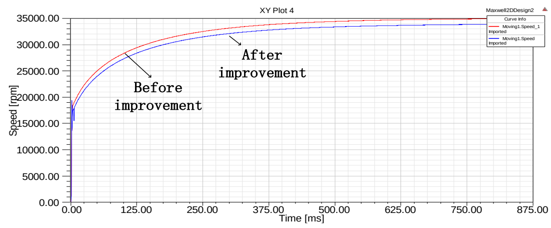

Fig. 13. Rotational speed waveform

Figures 14 and 15 show the waveforms of the motor before the parameter improvement. From the waveforms, it can be seen that the maximum value appears when the stator and rotor poles coincide, and thereafter it slowly decreases. The current peak value is close to 16 A, while the torque reaches 1.7 N·m. Excessive current and torque fluctuation will increase power consumption and reduce life span. Therefore, the improved parameters mainly focus on reducing the peak value.

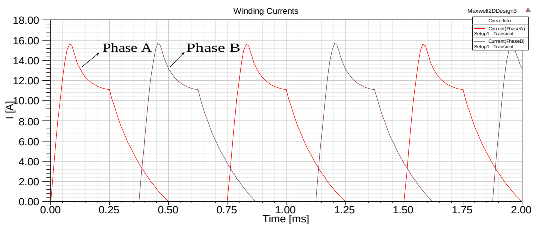

Fig. 14. Current waveform before improvement

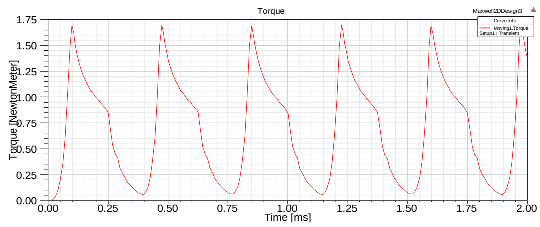

Fig. 15. Torque waveform before improvement

As shown in Figure 16, the iron core loss during motor operation. The magnetic flux in the motor flows on the iron core, and the iron core has a magnetoresistive effect on the magnetic flux. Through the analysis of motor structure in Section III and the selection of winding turns and air gap, the magnetic flux is at a better level, so the resulting hysteresis loss is controllable.

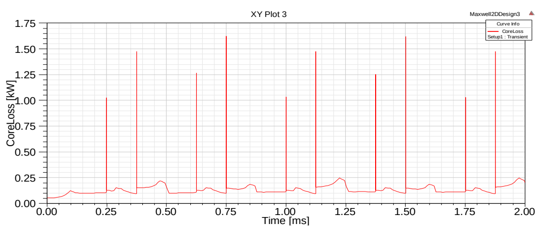

Fig. 16. Core loss

Figure 17 shows the external circuit loss of the motor. During the operation of the motor, the electric potential energy not only normally supplies the motor for operation, but also converts part of the energy into heat energy on the series resistance. The energy here will be consumed not only in the series resistance, but also in the internal resistance of the power supply and the internal resistance of the conductor, so this part of the loss should also be added to the motor analysis. As can be seen from Figure 17, the external circuit loss of switched reluctance motor is in a reasonable range compared with the normal operating power of the motor, so it will not cause large energy loss.

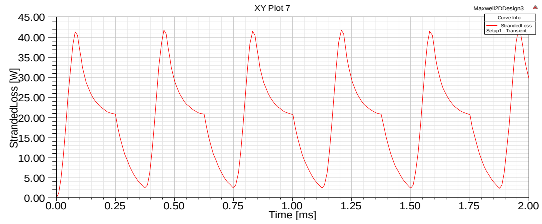

Fig. 17. stranded loss

Figures 18 and 19 show the improved motor waveforms. The peak current is reduced from 15.6 A before the improvement to 10.4 A, a drop of 33.3%. The fluctuation of electromagnetic torque T_e is reduced from 1.7 N·m before improvement to 0.76 N·m, torque ripple is reduced by 55.3%, and the effect of motor structure optimization is obvious.

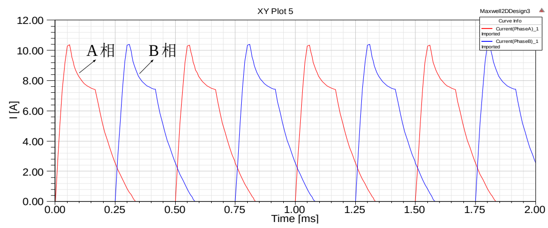

Fig. 18. Current waveform after improvement

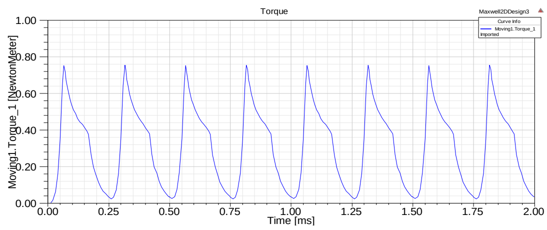

Fig. 19. Torque waveform after improvement

6. Summary

Aiming at the problems of the two-phase switched reluctance motor being unable to self-start and large torque ripple, an in-depth analysis is carried out from the perspective of the motor itself. Selecting 8/4 pole SRM, increasing the number of stator and rotor poles effectively reduces the torque dead zone, and according to the 8/4 motor, the parameters such as rotor outer diameter, stator yoke thickness and phase winding turns are reselected.

In addition, the two-phase SRM stepped air gap is analyzed through the ANSOFT static field, and it is determined that δ_e=0.55 and θ_{δ_e}=22.5°, and the self-starting ability is improved. On this basis, the finite element analysis method was used to build a two-dimensional field-circuit coupling simulation, and compared with the motor parameters before the improvement, the parameters after the improvement were in line with expectations. This time, only the optimization scheme of the motor body is studied. Next, the torque ripple suppression will be researched on the combination of the control strategy and the body.

References

[1] KLAUZ M, DORRELL D G. Eddy Current Effects in a Switched Reluctance Motor [J]. IEEE Transactions on Magnetics, 2006, 42 (10):3437-3439.

[2] ZHU Jin-bao, GAO Jian-ping, LIU Li-kun. Design and Performance Analysis of the Switched Reluctance Motor used to Power Tools[J]. The Journal of New Industrialization,2016,6(05):55-61.

[3] KIM J, KRISHNAN R. Novel Two-Switch-Based Switched Reluctance Motor Drive for Low-Cost High-Volume Applications[J].IEEE Transactions on Industry Applications, 2009, 45(4):1241-1248.

[4] ESKANDARI H, MIRSALIM M. An Improved 9/12 Two-Phase E-Core Switched Reluctance Machine[J]. IEEE Transactions on Energy Conversion, 2013, 28(4):951-958.

[5] FAIZ Jawad, PAKDELIAN Siavash. Finite-element analysis of a switched reluctance motor under static eccentricity fault[J]. IEEE Transactions on Magnetics, 2006, 42(8):2004-2008.

[6] WANG Jia-jun, SUN Jia-hao, ZHENG Zhi-yuan. Position control of SRM based on sliding-mode-learning neural networks[J]. Control and Decision, 2017, 32(06):1133-1136.

[7] WANG Qin-jian, DAI Yue-hong, SONG Lin, et al. Research on SRM Torque Ripple Suppression Based on Fuzzy Switching Angle Control[J]. Power Electronics, 2021, 55(03):29-31+93.

[8] SAHOO S K, PANDA S K, XU Jian-Xin. Indirect torque control of switched reluctance motors using iterative learning control[J]. IEEE Transactions on Power Electronics, 2005, 20(1):200-208.

[9] CAI Yan, ZHANG Dongxue. Simulation Study on Torque Ripple Reduction of a Switched Reluctance Motor Using New Rotor Tooth[J]. Transactions of China Electrotechnical Society, 2015, 30(S2):64-70.

[10] ZHANG Haijun, XU Weijie, WANG Shuhong, et al. Optimum Design of Rotor for High-Speed Switched Reluctance Motor Using Level Set Method[J].IEEE Transactions on Magnetics, 2014, 50(2):765-768.

[11] CHEN Hao, YAN Wenju. Flux Characteristics Analysis of a Double-Sided Switched Reluctance Linear Machine Under the Asymmetric Air Gap[J]. IEEE Transactions on Industrial Electronics, 2018, 65(12):9843-9852.

[12] CHEN Jiqing, XIAN Haolan, LAN Fengchong, et al. Structural Torque Ripple Suppression Method of Switched Reluctance Motor[J]. Journal of Mechanical Engineering, 2020, 56(20):106-119.

[13] YUAN Xiaoling, WANG Honghua. Calculation of phase current and electromagnetic force based on nonlinear inductance model of SRM[J]. Journal of Hohai University (Natural Sciences), 2006(06):705-708.

[14] SUN Qingguo, WU Jianhua, GAO Chun. Optimized Direct Instantaneous Torque Control for SRMs With Efficiency Improvement[J]. IEEE Transactions on Industrial Electronics, 2021, 68(3):2072-2082.

[15] SUN Huiqin, CUI Chen, HAN Jiawei, et al. Structure Optimization Design of Switched Reluctance Motor Based on Air Gap Change[J]. Micromotors, 2020, 53(10):5-10.

[16] YU Zhiyue, GAN Chun, CHEN Yu, et al. DC-Biased Sinusoidal Current Excited Switched Reluctance Motor Drives Based on Flux Modulation Principle[J].IEEE Transactions on Power Electronics, 2020, 35(10):10614-10628.

[17] LI Cunhe, WANG Guofeng, LI Yan, et al. Robust adaptive neural network control for switched reluctance motor drives[J]. Automatika, 2018, 59(1): 24-34.

[18] KIM Jaehyuck, KRISHNAN R. Novel Two-Switch-Based Switched Reluctance Motor Drive for Low-Cost High-Volume Applications[J].IEEE Transactions on Industry Applications, 2009, 45(4):1241-1248.

[19] LI Xiaoguang, SUN Huiqin, XUE Zhihong, et al. Study on torque algorithm of switched reluctance motor[J].Journal of Hebei University of Science and Technology, 2016, 37(06):594-600.

[20] CHEN Hao, NIE Rui, YAN Wenju. A Novel Structure Single-Phase Tubular Switched Reluctance Linear Motor[J]. IEEE Transactions on Magnetics, 2017, 53(11):1-4.

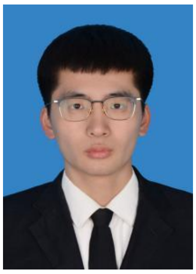

Yu Linhou is currently studying for a master's degree in the School of Electrical Engineering, Hebei University of Science and Technology, Shijiazhuang, China. He received a bachelor's degree from Hebei University of Science and Technology in 2019. His main research area is the control of switched reluctance motors.

Li Haonan is currently studying for a master's degree in the School of Electrical Engineering, Hebei University of Science and Technology. His main research field is the control and fault analysis of switched reluctance motors.